

## Electrochemical Behavior of Cu-9%Al-5%Ni-2%Mn Alloy in Chloride Media

Germano C. Serra, Assis V. Benedetti and Rodrigo Della Noce\*

Instituto de Química, Universidade Estadual Paulista, 14801-970 Araraquara-SP, Brasil

O comportamento eletroquímico da liga Cu-9%Al-5%Ni-2%Mn em diferentes concentrações de NaCl e valores de pH foi estudado por potencial em circuito aberto ( $E_{CA}$ ), voltametria cíclica e curvas de polarização. As curvas  $E_{CA}$  mostraram uma considerável influência da concentração de NaCl e do pH da solução nos valores de potencial de estado estacionário. Foi observado pelos perfis I/E que a variação da velocidade de varredura indicou a formação de um filme poroso de baixa condutividade o qual foi o responsável pelo aumento linear de corrente, devido à resistência da solução contida nos poros do filme. Com o intuito de investigar os produtos formados durante a varredura de potencial, o potencial foi mantido em diferentes valores de potencial aplicado dos voltamogramas cíclicos e analisado por MO, MEV e EDX. Em geral, foi observada a presença de precipitados de CuCl em potenciais aplicados iguais a 0,20; 0,85 e 0,00 V (vs. Ag/AgCl/KCl<sub>(3 mol.L<sup>-1</sup>)</sub>) e somente Cu em -0,70; -1,00 e -1,35 V. Nestes últimos, uma camada de Cu foi observada na superfície da liga devido à redução de cloreto cuproso. Este filme bloqueou o aparecimento dos picos de EDX relacionados aos outros metais presentes na liga. As curvas de polarização para a liga Cu-9%Al-5%Ni-2%Mn mostraram que  $E_{CA}$  variou conforme o pH da solução e a concentração de NaCl. Conforme a concentração de NaCl aumentou,  $E_{CA}$  tornou-se mais negativo para os três valores de pH estudados. Os coeficientes de Tafel foram calculados das curvas de polarização e os valores foram de 60 e 120 mV década<sup>-1</sup>, para a região anódica e catódica, respectivamente.

The electrochemical behavior of Cu-9%Al-5%Ni-2%Mn alloy in different NaCl concentrations and pHs was studied by means of open-circuit potential ( $E_{OC}$ ), cyclic voltammetry and polarization curves. The  $E_{OC}$  curves showed a considerable influence of NaCl concentration and solution pH in the steady-state potential values. It was observed by the I/E profiles that the scan rate variation indicated the formation of a porous film of low conductivity which was the responsible by the linear increase of current due to the solution resistance contained in the film pores. In order to investigate the products formed during the potential scan, the potential was held at different values of applied potential of the cyclic voltammogram and analyzed by OM, SEM and EDS. In general, it was noticed the presence of CuCl precipitates in applied potentials equals to 0.20, 0.85 and 0.00 V (vs. Ag/AgCl/KCl<sub>(3 mol.L<sup>-1</sup>)</sub>) and only Cu in -0.70, -1.00 and -1.35 V. In the latter cases, a Cu layer was observed on the alloy surface due to the cuprous chloride reduction. This film blocked the EDS peaks appearance related to the other metals present in the alloy. The polarization curves for Cu-9%Al-5%Ni-2%Mn showed that  $E_{OC}$  varied according to the solution pH and NaCl concentration. As the NaCl concentration increased the  $E_{OC}$  became more negative for the three pHs studied. The Tafel coefficients were calculated from the polarization curves and the values were 60 and 120 mV decade<sup>-1</sup>, for anodic and cathodic region, respectively.

**Keywords:** Cu-Al-Ni-Mn alloys, shape memory alloys, chloride media, potentiodynamic measurements

### Introduction

Much attention has been paid to Cu-based shape memory alloys (SMAs) because of their attractive properties related to the low cost, good corrosion resistance and easiness of processing.<sup>1-3</sup> Besides, these alloys

might offer the possibility of achieving transformation temperatures above 100 °C which make them interesting materials for high temperature applications.<sup>4</sup> Among these alloys, the Cu-Al-Ni alloys stand out in comparison to the Cu-Zn-Al<sup>5,6</sup> ones in view of their higher thermal stability. In addition, Recarte *et al.*<sup>5</sup> reported that the advantage of Cu-Al-Ni alloys from a technological point of view is their possible use at temperatures near 200 °C compared

\*e-mail: rodrnoce@iq.unesp.br

to the Cu-Zn-Al and Ti-Ni alloys whose maximum use temperatures are limited to 100 °C.

In this context, we have focused our work on the electrochemical behavior of Cu-Al-Ni alloys with the addition of small amounts of Mn, in particular the Cu-9%Al-5%Ni-2%Mn alloy. Morris and Lipe<sup>4</sup> demonstrated that Mn added in small concentrations to Cu-Al-Ni SMAs enhances the thermoelastic and pseudoelastic characteristics. Moreover, some papers<sup>4-8</sup> have only focused on the fabrication, mechanical properties and physical characterization of these alloys and electrochemical studies with Cu-Al-Ni-based alloys are so far still missing in the literature. The Cu-9%Al-5%Ni-2%Mn alloy electrochemical behavior was studied by means of potentiodynamic and open-circuit potential ( $E_{oc}$ ) measurements in different chloride concentrations and electrolyte pHs.

## Experimental

The Cu-9%Al-5%Ni-2%Mn alloy was prepared by melting the metals with purity higher than 99.9% using an Inductotherm Power-Track induction furnace under argon atmosphere in a graphite crucible. The melting temperature was around 1400 °C. The resulting ingot was machined to produce cylindrical rods (3 mm diameter) that were annealed at 850 °C for 120 h under argon atmosphere in an EDGCOM 3P furnace. After 120 h, the temperature in the furnace was gradually lowered and the samples were polished using SiC and diamond paste, etched and examined by optical microscopy, using a Nikon TS-100, and by scanning electron microscopy (SEM). The chemical analysis of the alloy was carried out by atomic absorption spectroscopy (AAS) and the nominal composition was Cu-9.55%Al-5.70%Ni-1.60%Mn. XRD measurements were performed in the  $2\theta$  range 10-100° with step size 0.05 and step time 1 s using a Siemens D5000 X-ray generator.  $\text{CuK}\alpha$  (1.54 Å) radiation was used at 40 kV and 30 mA with monochromator at the diffracted beam.

The electrochemical studies were carried out in a Tait-cell type at 25 °C. The electrochemical methods used were: open-circuit potential and potentiodynamic measurements using an EG&G PAR Model 273A Potentiostat/Galvanostat, coupled to an IBM-PC computer. The electrolyte was NaCl ranging from 0.001 to 0.3 mol L<sup>-1</sup> in three different pH values (3, 7 and 8.5) with constant ionic strength equal to 0.5 mol L<sup>-1</sup> adjusted with Na<sub>2</sub>SO<sub>4</sub>. The volume for each experiment was 50 mL in a deaerated aqueous solution. All solutions were prepared from analytical grade reagents (Merck) and Milli-Q water (18.2 MΩ cm).

An Ag/AgCl/KCl<sub>(3 mol L<sup>-1</sup>)</sub> electrode, connected to the solution through a Luggin capillary, was used as reference.

The auxiliary electrode was a Pt-spiral of geometric area 3.1 cm<sup>2</sup> and a Pt wire was connected to the reference by a capacitor of 0.1 μF to minimize the ohmic drop and noise.<sup>9</sup> Finally, a working electrode of the alloy was fixed at the bottom of the cell, exposing an area of 0.283 cm<sup>2</sup> to the solution.

## Results and Discussion

### Physical characterization

Figure 1 shows the optical micrographs of Cu-9%Al-5%Ni-2%Mn alloy annealed at 850 °C for 120-h. It can be noticed in both micrographs the  $\alpha$  phase in the grain interior, a Cu-based alloys characteristic, while in the grain boundary the ( $\alpha + \gamma$ ) pearlitic phase is observed, being  $\gamma$  an intermetallic compound such as Cu<sub>9</sub>Al<sub>4</sub>. The presence of  $\alpha$  and  $\gamma$  phases was confirmed by XRD as shown in Figure 3. The peaks referring to 43.13°, 49.98°, 73.22°, 88.57° and 93.55° were attributed to  $\alpha$  phase while the one observed in 44.38° was due to the  $\gamma$  phase. No other phases were noticed, indicating that Ni and Mn are totally dissolved into Cu matrix.

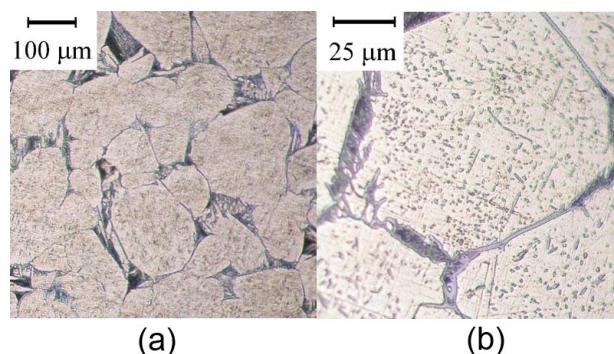


**Figure 1.** Optical micrographs of Cu-9%Al-5%Ni-2%Mn alloy annealed at 850 °C for 120 h.

### Open-circuit potential ( $E_{oc}$ )

Figure 2 depicts the open-circuit potential curves ( $E_{oc}$ ) for annealed Cu-9%Al-5%Ni-2%Mn alloy after 14 h at all NaCl concentrations and pHs studied. It can be noted that there are significant differences in the results, related to the immersion potential as well as the steady-state one, which in some cases was not reached even after 14 h experiment. At more acidic pH (pH 3) the potential decay is evidently noticed at the four different NaCl concentrations analyzed. This decay is probably explained in terms of dissolution of copper oxide film naturally formed into air, once Cu is the major element in the alloy composition. At neutral and alkaline pHs (pH 7 and 8.5) is seen that after the immersion,

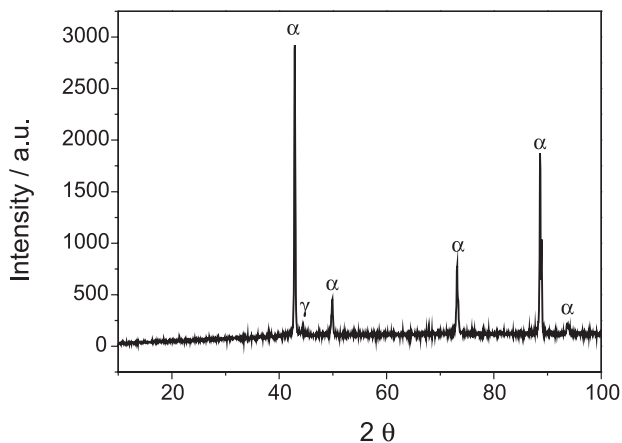


**Figure 2.** XRD pattern of annealed Cu-9%Al-5%Ni-2%Mn alloy.

the potential increases gradually up to reach the steady-state value. This indicates that the anodic oxidation of the alloy is taking place and leads to the formation of interfacial Cu species, possibly a copper oxide and CuCl passive layer. At higher NaCl concentration ( $0.3 \text{ mol L}^{-1}$ , Figure 2d), both effects, dissolution and oxidation, are hindered by the high electrolyte concentration that leads to a smaller variation in the observed steady-state potential for the three pH values.

### Cyclic voltammetry

The cyclic voltammograms for annealed Cu-9%Al-5%Ni-2%Mn alloy in NaCl solutions are shown in Figure 3. The I/E profiles were recorded at different scan rates from 1 up to  $20 \text{ mV s}^{-1}$  for three different pHs. The potential and current, both anodic and cathodic, for all I/E profiles displayed in Figure 3 are significantly affected by the used scan rate. For the others NaCl concentrations the cyclic voltammograms did not present two anodic peaks like in Figure 3, but only one probably attributed to the formation of CuCl and copper oxides. Basically, the I/E profiles in Figure 3 can be described as follows: in the positive scan there can be three different processes: (i) initial formation of cuprous oxide,  $\text{Cu}_2\text{O}$ ; (ii) followed by a formation of a cuprous chloride film,  $\text{CuCl}^{10}$  and (iii) oxidation of Cu(I) to Cu(II). The formation of a porous film and with low conductivity is the responsible by the linear increase of current due to the solution resistance contained in the pores of this film. This is also supported by the fact that right after the coverage of the electrode surface, the charge transfer resistance increases and the current decreases. In the negative scan, a small intensity anodic peak appears before 0 V, which is associated to the

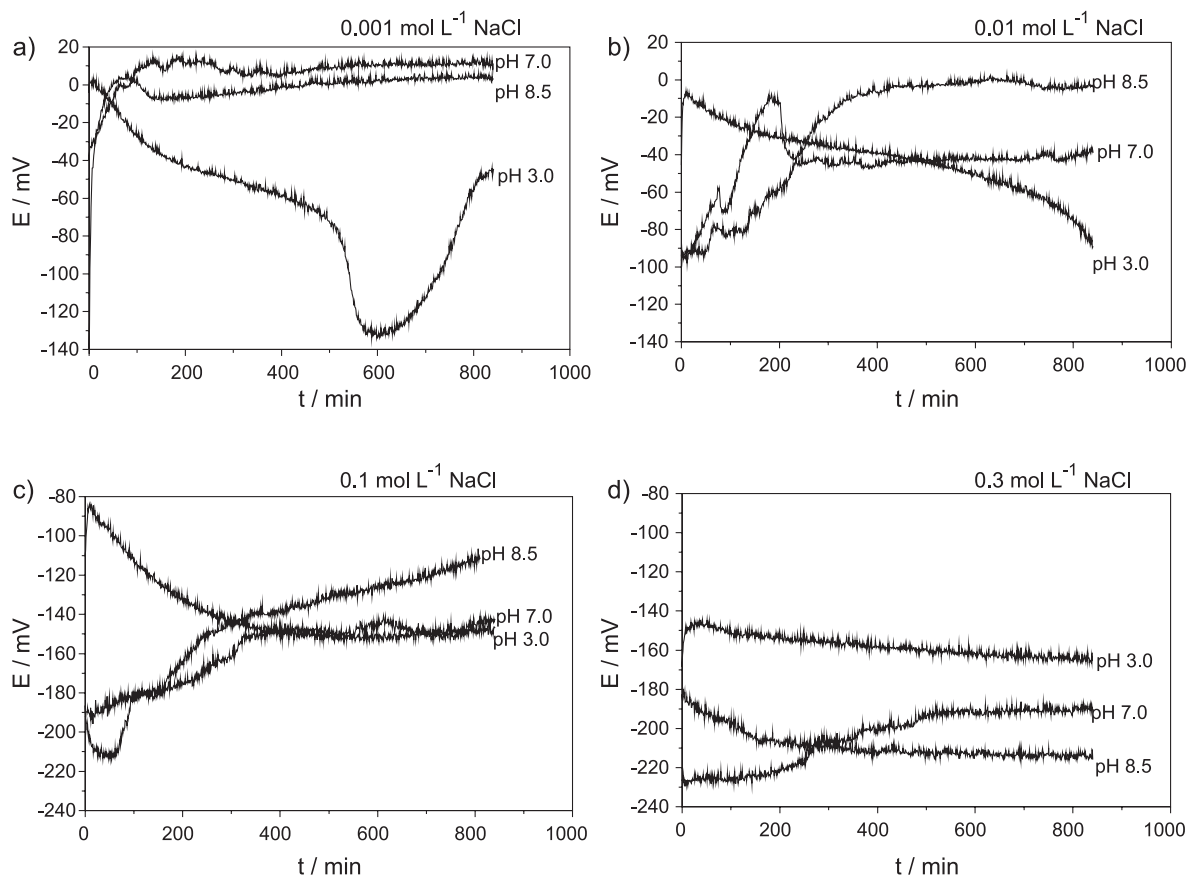


**Figure 3.** Open-circuit potential ( $E_{oc}$ ) vs. time curves for annealed Cu-9%Al-5%Ni-2%Mn alloy in NaCl solution: a)  $0.001 \text{ mol L}^{-1}$ , b)  $0.01 \text{ mol L}^{-1}$ , c)  $0.1 \text{ mol L}^{-1}$  and d)  $0.3 \text{ mol L}^{-1}$ .

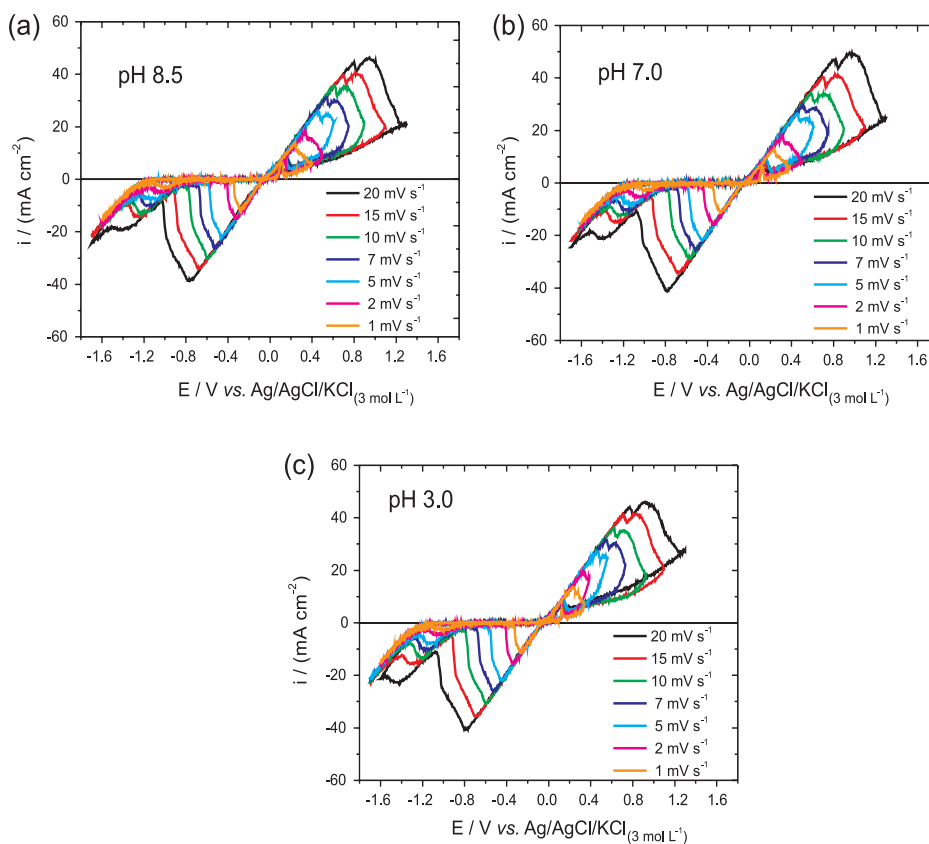
copper oxidation as a consequence of the film breakdown, exposing the metal to the electrolyte. Continuing the scan, it can be observed a high intensity cathodic peak at  $-0.6$  V for  $10 \text{ mV s}^{-1}$  for example, whose linear increase of current starts at  $-0.09$  V and reaches a maximum with consequent decrease up to reduce the whole CuCl film at *ca.*  $-0.8$  V. From this point, it shows up another small intensity peak at  $-1.2$  V that possibly corresponds to the reduction of oxides formed on the alloy surface.

In order to investigate the products formed during the potential scan, a cyclic voltammogram was performed for different regions of applied potential as shown in Figure 4. In this voltammogram are numbered some regions where the scan was held, applying the specific potential for one minute. After that, the sample was removed from the solution and rinsed with deionized water for posterior analysis of surface by OM, SEM and energy dispersive spectrometry (EDS). At  $0.20$  and  $0.80$  V the samples were also rinsed with 50% HCl. These analyses were carried out in order to observe and to characterize the precipitates, especially salts that might be formed or decompose on alloy surface during the potential scan. The CV shows an anodic peak ( $0.85$  V) that corresponds to the formation of Cu(I) salts which are reduced in the first peak of the reverse process ( $-0.70$  V).

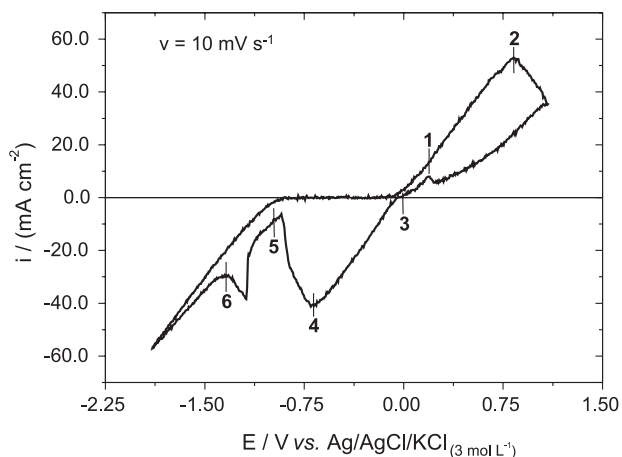
The cathodic peak between  $-1.00$  and  $-1.35$  V is related to the reduction of copper oxides to Cu(0), followed by an increase of the cathodic current attributed to the region where the hydrogen evolution occurs.

Figure 5 exhibits the OM and SEM images of annealed Cu-9%Al-5%Ni-2%Mn alloy after applying  $0.20$  and  $0.85$  V, respectively. The OM images show the precipitates formation on the alloy surface, predominantly triangle shapes, characteristic of the copper(I) chloride formation.<sup>7,8</sup> Comparing the two images, it can be observed a smaller amount of precipitates in Figure 5a, because at  $0.20$  V is the beginning of the oxidation peak, where the precipitates formation starts to take place. The different amount of formed precipitates on the alloy surface at  $0.20$  and  $0.85$  V is clearly noticed by SEM; in the latter, the surface is almost totally covered by copper(I) chloride and it is also possible to observe a better geometry of CuCl precipitates. The EDS analysis evidenced this behavior showing the Cl presence enhanced at  $0.85$  V due to the more intense CuCl formation.

The same procedure was made for the OM and SEM images of annealed Cu-9%Al-5%Ni-2%Mn shown in Figure 6, but in this case after holding the potential at the specific values, the samples were rinsed with 50% HCl solution instead of only deionized water. It is seen that in all

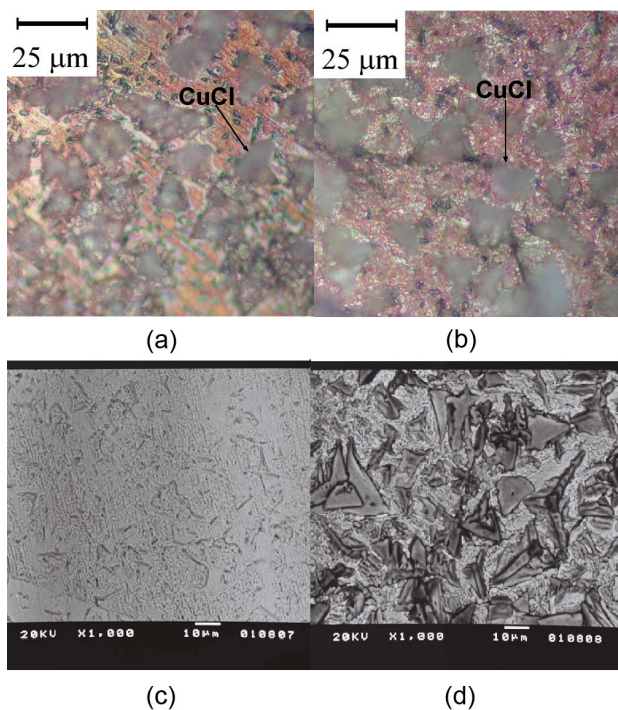


**Figure 4.** Cyclic voltammograms for annealed Cu-9%Al-5%Ni-2%Mn alloy in  $0.3 \text{ mol L}^{-1}$  NaCl solution at different scan rates: a) pH 3.0, b) pH 7.0 and c) pH 8.5. (Color online).



**Figure 5.** Cyclic voltammogram for annealed Cu-9%Al-5%Ni-2%Mn alloy obtained at  $v = 10 \text{ mV s}^{-1}$  in  $0.5 \text{ mol L}^{-1}$  NaCl at pH 7.

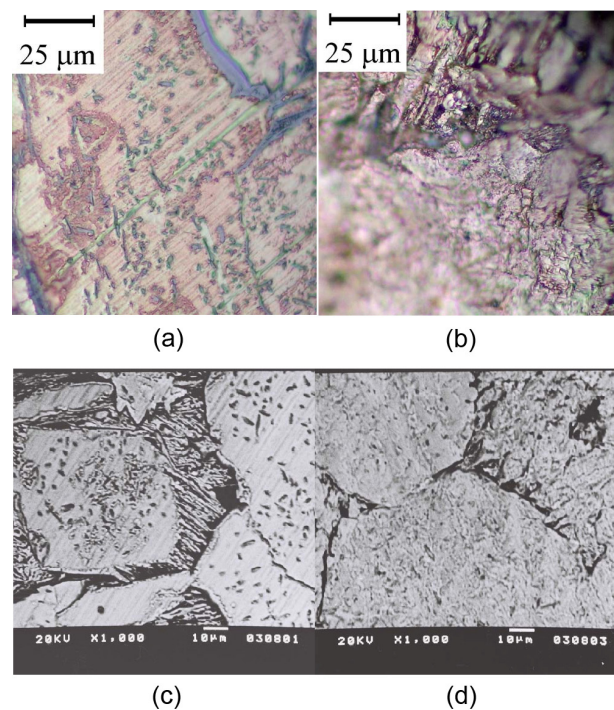
images there are no precipitates characteristic of copper(I) chloride, because the HCl dissolved these precipitates of the alloy surface, exposing the alloy microstructure. However, the alloy presents small precipitates rich in nickel and aluminum whose are typical of this kind of alloy. These observations were confirmed by the EDS analysis (not shown) that exhibited Ni and Al peaks more intense compared to the samples described in Figure 5. In addition, it was observed the enhancement of Cu peaks and consequent disappearance of Cl peak, evidencing that the copper(I) chloride dissolution took place.



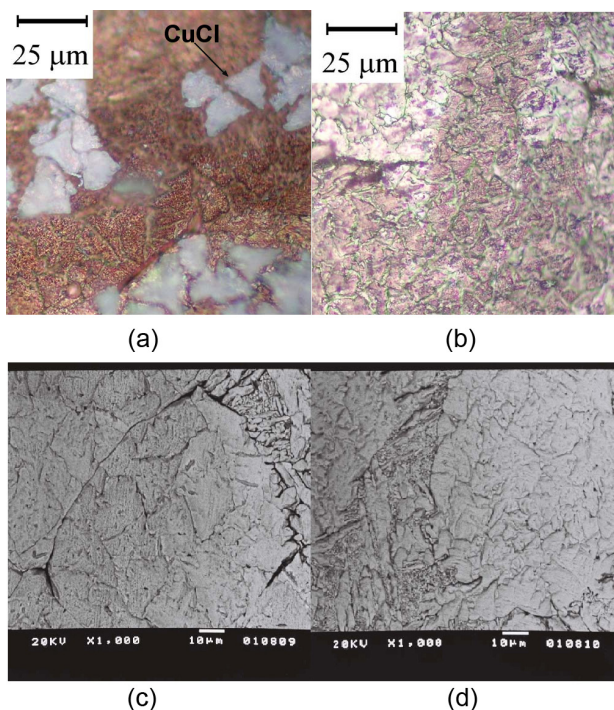
**Figure 6.** OM (a,b) and SEM (c,d) of annealed Cu-9%Al-5%Ni-2%Mn right after applying 0.20 V (a,c) and 0.85 V (b,d) of Figure 4 (Samples rinsed with deionized water).

Figure 7 displays the OM and SEM images of annealed Cu-9%Al-5%Ni-2%Mn alloy after applying 0.00 and  $-0.70 \text{ V}$ . At  $0.00 \text{ V}$  is located the beginning of the reduction peak, therefore, it is observed in Figures 7a and 7c the presence of little precipitates on the alloy surface, because the copper(I) chloride reduction is not complete yet. At  $-0.70 \text{ V}$  (Figures 7b and 7d), no precipitates on the alloy surface are observed as a consequence of the CuCl film that was completely reduced to metallic copper. The EDS (not shown) related to the Figures 7a and 7c exhibited a very intense Cl peak followed by a Cu peak. Al, Ni and Mn showed low intensity peaks in the respective spectrum. The EDS associated to the Figures 7b and 7d did not display Cl peaks, on the other hand, very intense Cu peaks were observed as a consequence of Cu deposition and also of CuCl reduction. As the alloy surface was completely covered by copper, the peaks corresponding to the other elements were not noticed in the EDS spectrum.

Finally, OM and SEM images obtained after applying  $-1.00$  and  $-1.35 \text{ V}$  were analyzed and are shown in Figure 8. All images reveal only the alloy microstructure and no precipitates on the surface are noticed. This behavior was expected, because in these regions, the CuCl precipitates formed previously were totally reduced to metallic copper. The EDS analysis revealed that in both cases Cu presents a very intense peak and Cl peaks were not identified in the respective spectra. The Cu layer



**Figure 7.** OM (a,b) and SEM (c,d) of annealed Cu-9%Al-5%Ni-2%Mn right after applying 0.20 V (a,c) and  $0.85 \text{ V}$  ( b,d) of Figure 4 (samples rinsed with 50% HCl solution).



**Figure 8.** OM (a,b) and SEM (c,d) of annealed Cu-9%Al-5%Ni-2%Mn right after applying 0.00 V (a,c) and -0.70 V (b,d) of Figure 4.

formed on the electrode surface due to its deposition during the cathodic scan at -1.00 and -1.35 V, impedes the peaks appearance referring to the other metals present in the alloy and consequently very low intensity peaks are observed for these elements.

#### Polarization curves

Figure 9 presents the polarization curves obtained in 0.3 mol L<sup>-1</sup> NaCl solution with three different pHs. The Tafel plots were recorded at 0.166 mV s<sup>-1</sup>, starting from the  $E_{OC}$  to the negative part (up to -0.150 V/ $E_{OC}$ ) and then restarting from  $E_{OC}$  to the positive one (up to +0.450 V/ $E_{OC}$ ). The parameters extracted from the curves in Figure 9 as well as from the others NaCl concentrations and pHs are listed in Table 1. The  $E_{OC}$  values varied according to the solution pH and NaCl concentration. In general, as the NaCl concentration increases the  $E_{OC}$  becomes more negative for the three pHs. It can be seen that in all curves in the negative scan there is a limit current density ( $i_{C,Limit}$ ) of about 30  $\mu\text{A cm}^{-2}$  due to ions or oxygen transport to the electrode surface. If the Tafel coefficients are calculated for both regions, anodic ( $b_a$ ) and cathodic ( $b_c$ ), the values are 60 and 120 mV decade<sup>-1</sup>, respectively, for all NaCl concentrations and pHs, showing that these two features do not affect the Tafel anodic coefficient. This  $b_a$  value is similar to the one obtained for some authors<sup>11,12</sup> for pure Cu. Awad *et al.*<sup>11</sup> explained the obtained  $b_a$  (60 mV decade<sup>-1</sup>) in terms of a

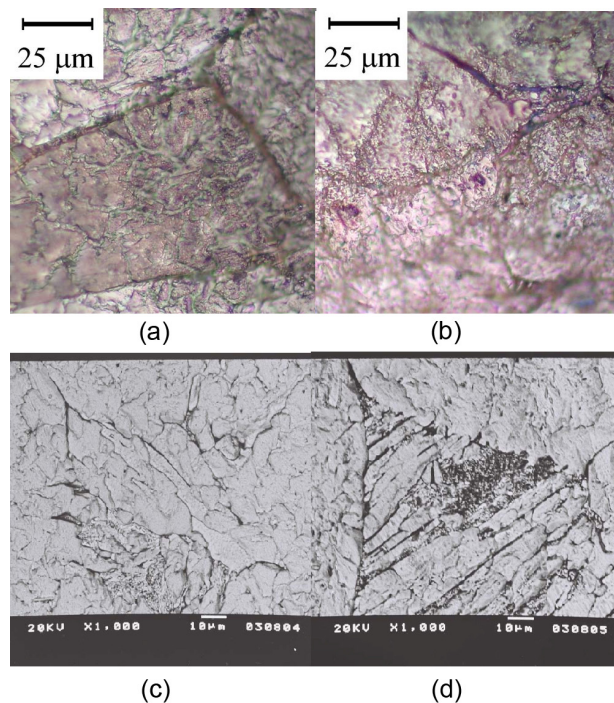
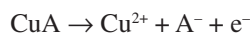


**Figure 9.** OM (a,b) and SEM (c,d) of annealed Cu-9%Al-5%Ni-2%Mn right after applying -1.00 V (a,c) and -1.35 V (b,d) of Figure 4.

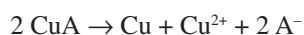
**Table 1.** Parameters obtained from the polarization curves for annealed Cu-9%Al-5%Ni-2%Mn alloy in different NaCl concentrations and pHs

pH	NaCl / (mol L <sup>-1</sup> )	$E_{OC}$ / mV	$i_{C,Limit}$ / ( $\mu\text{A cm}^{-2}$ )	$i_{Corr}$ / ( $\mu\text{A cm}^{-2}$ )
3	0.3	-195	27	7.7
	0.1	-130	27	1.95
	0.01	-40	61	8.45
7	0.001	-43	38	3.15
	0.3	-235	26	2.7
	0.1	-170	22	0.54
8.5	0.01	-90	27	0.55
	0.001	-75	21	0.98
	0.3	-230	32	3.6
	0.1	-183	20	1.40
	0.01	-120	18	0.10
	0.001	-80	31	0.53

mechanism where the global reaction rate is controlled by two simultaneous processes; one electrochemical oxidation reaction that involves the specie CuA (A represents the anions Cl<sup>-</sup>, NO<sub>3</sub><sup>-</sup> or SO<sub>4</sub><sup>2-</sup>)



and a disproportionation reaction:



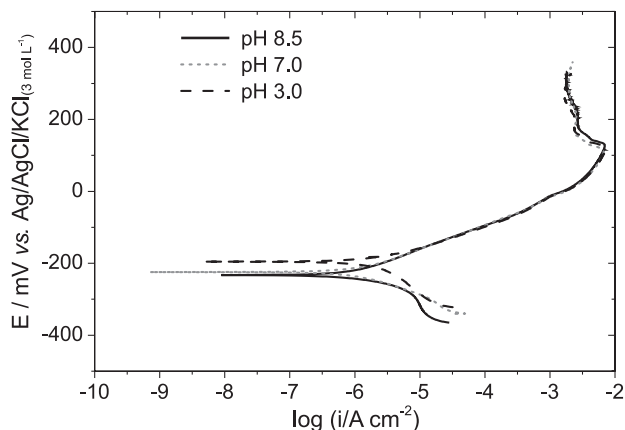


**Figure 10.** Polarization curves for annealed Cu-9%Al-5%Ni-2%Mn alloy in  $0.3 \text{ mol L}^{-1}$  NaCl at different pHs.

The same  $b_a$  value has been obtained for Cu-Al alloys<sup>13,14</sup> with Al compositions in the range 8 to 13 wt.%. Sury and Oswald<sup>13</sup> reported that Cu-Al alloys in chloride media showed a Tafel anodic coefficient equal to  $60 \text{ mV decade}^{-1}$ , supposing that the alloys dissolution reaction is governed by diffusion controlled process.

## Conclusions

The electrochemical behavior of Cu-9%Al-5%Ni-2%Mn alloy in chloride media at different pHs was studied by means of open-circuit potential, cyclic voltammetry and polarization curves. The  $E_{OC}$  curves showed a considerable influence of NaCl concentration and solution pH in the steady-state potential values. The variation of scan rate in the cyclic voltammograms of Cu-9%Al-5%Ni-2%Mn alloy indicated the formation of a porous film and with low conductivity which is the responsible by the linear increase of current due to the solution resistance contained in the film pores. Holding the potential in different values of applied potential of the alloy cyclic voltammogram, it was possible to observe by OM, SEM and EDS the different products formed on the alloy surface according to the applied potential. In general, it was noticed the presence of CuCl precipitates in applied potentials equals to 0.20, 0.85 and 0.00 V (vs. Ag/AgCl/KCl<sub>(3 mol L<sup>-1</sup>)</sub>) and only Cu in -0.70, -1.00 and -1.35 V. In the latter cases, a Cu layer was observed on the alloy surface due to the cuprous chloride reduction. The polarization curves for Cu-9%Al-5%Ni-2%Mn

showed that  $E_{OC}$  values varied according to the solution pH and NaCl concentration. In general, as the NaCl concentration increased the  $E_{OC}$  became more negative for the three pHs studied. The solution pH had a significant influence on the corrosion current density ( $i_{Corr}$ ). The Tafel coefficients were calculated from the polarization curves and the values were 60 and  $120 \text{ mV decade}^{-1}$ , for anodic and cathodic region, respectively.

## Acknowledgments

The authors would like to thank the Brazilian Agencies, CNPq (Proc. No. 300728/2007-7), CAPES and FAPESP for financial support.

## References

- Li, Z.; Pan, Z. Y.; Tang, N.; Jiang, Y.B.; Liu, N.; Fang, M.; Zheng, F.; *Mater. Sci. Eng., A* **2006**, *417*, 225.
- Xiao, Z.; Li, Z.; Fang, M.; Xiong, S.; Sheng, X.; Zhou, M.; *Mater. Sci. Eng., A* **2008**, *488*, 266.
- Zak, G.; Kneissl, A. C.; Zatulskij, G.; *Scr. Mater.* **1996**, *34*, 363.
- Morris, M. A.; Lipe, T.; *Acta Metall. Mater.* **1994**, *42*, 1583.
- Recarte, V.; Hurtado, I.; Herreros, J.; N6, M. L.; Juan, J. S.; *Scr. Mater.* **1996**, *34*, 255.
- Recarte, V.; Perez-Landazabal, J. I.; Ibarra, A.; *Mater. Sci. Eng., A* **2004**, *378*, 238.
- Tatar, C.; Zengin, R.; *Thermochim. Acta* **2005**, *433*, 56.
- Huang, Y. T.; Ho, M. K.; *Acta Metall. Mater.* **1992**, *40*, 4959.
- Garreau, D.; Saveant, J. M.; Binh, E. S. K.; *J. Electroanal. Chem.* **1978**, *89*, 427.
- Benedetti, A. V.; Sumodjo, P. T. A.; Nobe, K.; Cabot, P. L.; Proud, W. G.; *Electrochim. Acta* **1995**, *40*, 2657.
- Awad, S. A.; Kamel, K. H.; ElHadi, Z. A.; Bayumi, H. A.; *J. Electroanal. Chem.* **1986**, *199*, 34.
- Crundwell, F. K.; *Electrochim. Acta* **1992**, *37*, 2707.
- Sury, P.; Oswald, H. R.; *Corros. Sci.* **1972**, *12*, 77.
- Noce, R. D.; Fugivara, C. S.; Barelli, N.; Benedetti, A. V.; *Port. Electrochim. Acta* **2003**, *21*, 117.

Received: September 22, 2009

Web Release Date: April 22, 2010

FAPESP has sponsored the publication of this article.